# DARTFlo - Discrete Adjoint for Rapid Transonic Flows

Theory manual

**Adrien Crovato**

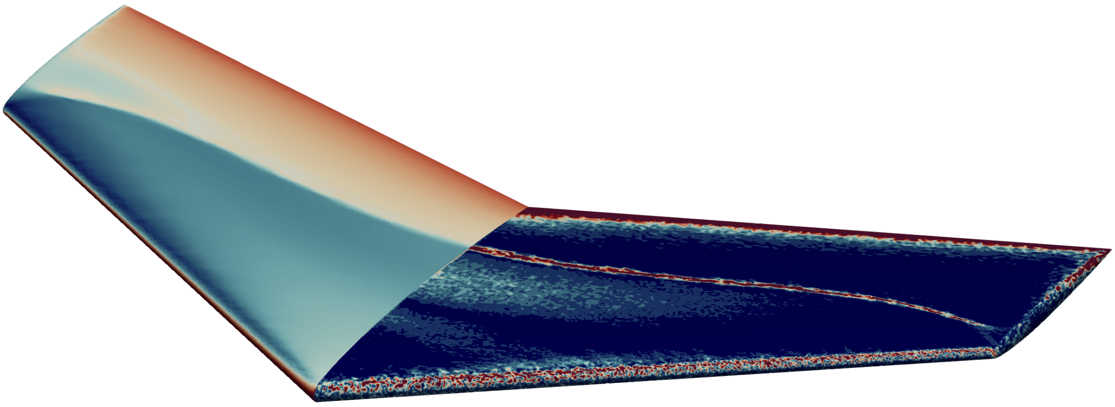

Department of Aerospace & Mechanical Engineering

# Abstract

This document provides the mathematical formulation of the main equations implemented in DARTFlo [1], version 1.1.0 (October 2021). For more detailed information about the original implementation, refer to the author's PhD thesis [2].

This quick reference theory manual is organized as follows. Section 1 presents the formulation of the discretized full potential equation and the mesh morphing laws. Section 2 presents the formulation of their partial gradients. Finally, section 3 presents the direct and adjoint solution procedures.

# Contents

# 1 Model equations

This section presents the formulation of the discretized full potential model and mesh morphing laws.

## 1.1 Full potential

This section details the formulation of the full potential equation written in residual form, and of the aerodynamic loads.

### 1.1.1 Residuals

The steady full potential equation is derived form the Navier-Stokes equations by assuming that the fluid is inviscid, and that the flow is steady and isentropic. As a consequence, the vorticity is conserved. Since the freestream flow is irrotational, the whole flow is therefore irrotational and the velocity derives from a potential $\phi$. Considering a domain $\Omega$ enclosed by a surface $\Gamma = \Gamma_\mathrm{f} \cup \Gamma_\mathrm{b}$, as depicted in Figure 1.1, the full potential equation can be written in weak form as,

$$\int_\Omega \rho\nabla\phi\cdot\nabla\psi\,dV - \int_\Gamma \overline{\rho\nabla\phi}\cdot\hat{\mathbf{n}}\psi\,dS = 0, \qquad \forall\psi\in\Omega, \tag{1.1}$$

where $\psi$ is a test function, $\hat{\mathbf{n}}$ is the unit vector normal to $\Gamma$ pointing inwards, and where the density $\rho$ is given by the isentropic flow relationship,

$$\rho = \rho_\infty\left[1+\frac{\gamma-1}{2}M_\infty^2\left(1-|\nabla\phi|^2\right)\right]^{\frac{1}{\gamma-1}}. \tag{1.2}$$

In Equation 1.2, $\rho_\infty$ is the freestream density, $\gamma$ is the heat capacity ratio and $M_\infty$ is the freestream Mach number. Note that the term $|\nabla\phi|$ in Equation 1.2, which is the magnitude of the total velocity, has been normalized by the freestream velocity. An important limitation of the nonlinear potential equation is the isentropicity assumption, which restricts its use to transonic flows with embedded weak shocks only. A common upper limit for the local normal Mach number upstream of the shock is $M_n < 1.3$ [3].

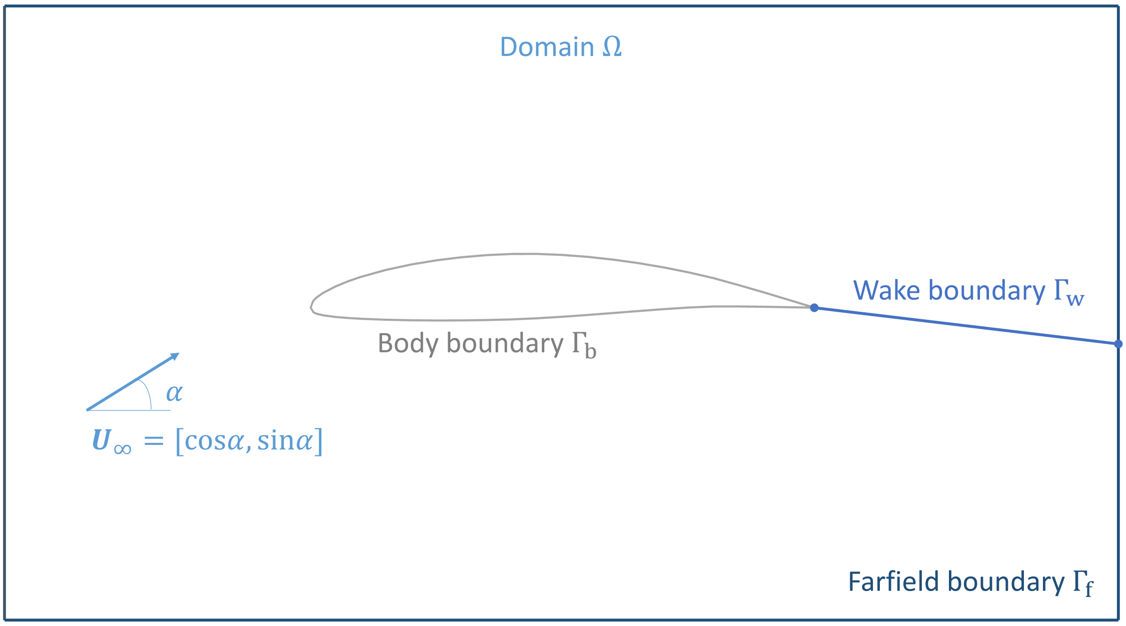
Domain Ω
Wake boundary $\Gamma_w$
Body boundary $\Gamma_b$
$\alpha$
$U_\infty = [\cos\alpha, \sin\alpha]$
Farfield boundary $\Gamma_f$

Figure 1.1: Typical domain used for a finite element computation, illustrated in two dimensions for simplicity.

The boundary surface $\Gamma$ is split into a farfield boundary $\Gamma_\mathrm{f}$, and a body boundary $\Gamma_\mathrm{b}$, as depicted in Figure 1.1, onto which Neumann boundary conditions are applied. Such boundary conditions impose a flux through the boundaries of the domain and are naturally recovered in the second term of the weak formulation of the full potential equation 1.1. Since the derivative of the potential is the velocity, the weak form of the Neumann boundary condition can be written as

$$\begin{aligned} &\int_{\Gamma_\mathrm{f}} \overline{\rho \nabla \phi} \cdot \hat{\mathbf{n}} \psi \, dS = \int_{\Gamma_\mathrm{f}} \rho_\infty \mathbf{U}_\infty \cdot \hat{\mathbf{n}} \psi \, dS, \qquad \forall \psi \in \Gamma_\mathrm{f} \\ &\int_{\Gamma_\mathrm{b}} \overline{\rho \nabla \phi} \cdot \hat{\mathbf{n}} \psi \, dS = 0, \qquad \forall \psi \in \Gamma_\mathrm{b} \end{aligned} \tag{1.3}$$

where $\mathbf{U}_\infty$ is the freestream velocity vector given by,

$$\mathbf{U}_\infty = \begin{bmatrix} \cos\alpha\cos\beta \\ \sin\beta \\ \sin\alpha\cos\beta \end{bmatrix}, \tag{1.4}$$

and where $\alpha$ is the angle of attack and $\beta$ is the angle of sideslip. Additionally, the Kutta condition needs to be enforced to allow potential flows to produce aerodynamic loads. This is accomplished by creating a flat wake sheet, denoted $\Gamma_\mathrm{w}$, extending from the trailing edge of any lifting body to the farfield boundary located downstream of these bodies, as depicted in Figure 1.1. The unknown potential value is discontinuous across the wake, and two boundary conditions are applied to restore the continuity in the flow variables. The first condition prescribes the equality of the mass flux across the wake,

$$\int_{\Gamma_\mathrm{w}} [\![\rho\nabla\phi \cdot \hat{\mathbf{n}}]\!]\psi \, dS = 0, \qquad \forall\psi \in \Gamma_{\mathrm{w,l}}, \tag{1.5}$$

and the second condition prescribes the equality of the pressure across the wake,

$$\int_{\Gamma_\mathrm{w}} [\![|\nabla\phi|^2]\!]\Psi \, dS = 0, \qquad \forall\Psi \in \Gamma_{\mathrm{w,u}}, \tag{1.6}$$

where $\Psi$ is a stabilized test function, the double square bracket indicates a jump between the quantities on the upper and lower sides of the wake, and the subscripts $\mathrm{u}$ and $\mathrm{l}$ refer to the upper and lower sides of the wake, respectively.

Finally, supersonic regions of the flow need to be stabilized. The physical density is upwinded and replaced by,

$$\tilde{\rho} = \rho - \mu(\rho - \rho_\mathrm{U}), \tag{1.7}$$

where $\rho_\mathrm{U}$ is the density evaluated at an upwind point, and where the switching function is defined as

$$\mu = \mu_\mathrm{C} \max\left(0, 1 - \frac{M_\mathrm{C}^2}{M^2}\right). \tag{1.8}$$

The parameters $\mu_\mathrm{C}$, which controls the amplification of the density bias, and $M_\mathrm{C}$, which controls the extent of the region where the bias is applied, are controlled by the numerical scheme. They are initialized to $2$ and $0.92$ in order to produce strong stabilization over a large portion of the flow. As the solution converges, they are varied to $1$ and $0.95$. These final values were chosen from the literature, as they are suitable for most cases. The parameters are updated each time the relative residual of the full potential equation drops below $10^{-2}$.

The domain $\Omega$ and its boundary $\Gamma$ are discretized using continuous Galerkin finite elements. An unstructured grid strategy is chosen in order to easily mesh three-dimensional complex shapes. The potential, test functions and coordinates are expressed as

$$\begin{aligned} \phi &= N_i\phi_i, \\ \psi &= N_i\psi_i, \\ x_k &= N_i x_{i,k} \end{aligned} \tag{1.9}$$

where $N_i$ are the shape functions associated to an element, and interpolate the nodal values $\phi_i$ and $\psi_i$ of the potential and the test functions, as well as the nodal coordinates $x_{i,k} = [x, y, z]_i$, on that element. Note that the shape functions are expressed locally on each element as,

$$N_i = N_i(\xi_j) = N_i\left([\xi, \eta, \zeta]\right), \tag{1.10}$$

where $\xi_j$ is the vector of coordinates attached to the reference frame of an element. The weak form of the full potential equation 1.1 must hold for any test function $\psi$. It can then be discretized and rewritten in residual form,

$$\mathbf{R}_\phi = \sum_{\mathrm{e}} \int_{\Omega_\mathrm{e}} \tilde{\rho}_\mathrm{e} \nabla N_j \phi_j \cdot \nabla N_i \, dV_\mathrm{e} - \sum_{\mathrm{e}} \int_{\Gamma\mathrm{e}} \overline{\rho \nabla \phi}_\mathrm{e} \cdot \hat{\mathbf{n}}_\mathrm{e} N_i \, dS_\mathrm{e} \\ = 0, \tag{1.11}$$

where the subscript $\mathrm{e}$ refers to elemental quantities. The associated Neumann boundary conditions 1.3 become

$$\begin{aligned} \sum_{\mathrm{e}} \int_{\Gamma_{\mathrm{f_e}}} \overline{\rho \nabla \phi}_\mathrm{e} \cdot \hat{\mathbf{n}}_\mathrm{e} N_i \, dS_\mathrm{e} &= \sum_{\mathrm{e}} \int_{\Gamma_{\mathrm{f_e}}} \rho_\infty \mathbf{U}_\infty \cdot \hat{\mathbf{n}}_\mathrm{e} N_i \, dS_\mathrm{e}, \\ \sum_{\mathrm{e}} \int_{\Gamma_{\mathrm{b_e}}} \overline{\rho \nabla \phi}_\mathrm{e} \cdot \hat{\mathbf{n}}_\mathrm{e} N_i \, dS_\mathrm{e} &= 0. \end{aligned} \tag{1.12}$$

The equality of mass flux across the wake 1.5 is enforced on the lower wake nodes as,

$$\sum_{\mathrm{e}} \int_{\Gamma_{\mathrm{w,l_e}}} \tilde{\rho}_\mathrm{e} \nabla N_j \phi_j \cdot \nabla N_i \, dS_\mathrm{e} - \sum_{\mathrm{e}} \int_{\Gamma_{\mathrm{w,u_e}}} \tilde{\rho}_\mathrm{e} \nabla N_j \phi_j \cdot \nabla N_i \, dS_\mathrm{e} = 0, \tag{1.13}$$

and the equality of the pressure 1.6 is enforced on the upper wake nodes as,

$$\sum_{\mathrm{e}} \int_{\Gamma_{\mathrm{w_e}}} \left( [\nabla \phi \cdot \nabla N_j \phi_j]_{\mathrm{w,u}} - [\nabla \phi \cdot \nabla N_j \phi_j]_{\mathrm{w,l}} \right) \left( N_i + \frac{h}{2} \tilde{U}_{\infty,k} \partial_{x_k} N_i \right)_{\mathrm{w,u}} dS_\mathrm{e} = 0. \tag{1.14}$$

where $h$ is the square root of the cell area and $\tilde{\mathbf{U}}_\infty = [1,0,0]$.

### 1.1.2 Functional

The total aerodynamic load vector is obtained by multiplying the aerodynamic total load coefficient $\mathbf{C_F}$ by the freestream dynamic pressure,

$$\mathbf{F} = \frac{1}{2} \rho_\infty u_\infty^2 S_{\mathrm{ref}} \mathbf{C_F}. \tag{1.15}$$

The resulting aerodynamic load coefficient is computed by integrating the normalized pressure coefficient on the body surface,

$$\mathbf{C_F} = \frac{1}{S_{\mathrm{ref}}} \int_{\Gamma_\mathrm{b}} C_p \hat{\mathbf{n}} \, dS, \tag{1.16}$$

where $S_{\mathrm{ref}}$ is a reference area, and where the pressure coefficient is given by

$$C_p = \frac{2}{\gamma M_\infty^2} \left( \rho^\gamma - 1 \right). \tag{1.17}$$

The aerodynamic load coefficients are obtained by projecting $\mathbf{C_F}$ on the lift and drag directions, yielding

$$C_L = \mathbf{C_F} \cdot \mathbf{e_L}, \qquad C_D = \mathbf{C_F} \cdot \mathbf{e_D}, \tag{1.18}$$

where the directions are defined with respect to the angle of attack $\alpha$, and the angle of sideslip $\beta$,

$$\mathbf{e_L} = \begin{bmatrix} -\sin\alpha \\ 0 \\ \cos\alpha \end{bmatrix}, \qquad \mathbf{e_D} = \begin{bmatrix} \cos\alpha\cos\beta \\ \sin\beta \\ \sin\alpha\cos\beta \end{bmatrix}. \tag{1.19}$$

## 1.2 Mesh deformation

This section details the formulation of the linear elasticity laws written in residual form, driving the mesh morphing.

### 1.2.1 Residuals

An efficient way to deform the grid for the kind of wing deflections considered in practical aeroelasticity, is to use linear elasticity theory. The grid is assumed to behave like an elastic body, rigid near the deforming boundaries, and flexible elsewhere. Moreover, the linear elasticity equations can be easily solved by the finite element method, and require little supplementary implementation work.

For an elastic solid, the equilibrium between the internal and external forces can be written in weak form as

$$\int_\Omega \nabla\boldsymbol{\sigma}\cdot\nabla\psi\,dV - \int_\Gamma \overline{\nabla\boldsymbol{\sigma}}\cdot\hat{\mathbf{n}}\psi\,dS = \int_\Omega \mathbf{f}\psi\,dV, \qquad \forall\psi\in\Omega, \tag{1.20}$$

where the internal stress $\boldsymbol{\sigma}$ can be related to the displacement $\Delta\mathbf{x}$ using Hooke's constitutive law for linear isotropic solids,

$$\boldsymbol{\sigma} = \frac{E\nu}{2(1+\nu)(1-2\nu)}\mathrm{tr}\left(\nabla\left(\Delta\mathbf{x}\right)+\nabla\left(\Delta\mathbf{x}\right)^{\mathrm{T}}\right)\mathbf{I} + \frac{E}{2(1+\nu)}\left(\nabla\left(\Delta\mathbf{x}\right)+\nabla\left(\Delta\mathbf{x}\right)^{\mathrm{T}}\right). \tag{1.21}$$

The Young modulus $E$ and the Poisson's ratio $\nu$ are constitutive parameters. In the present work, they are set to $1/V$ and $0$, respectively, as suggested by Dwight [4]. As a result, the mesh behaves as a linear elastic solid, rigid close to the wing where the elements are small, and flexible in the farfield where the elements are large. Note that, in the context of mesh deformation, the external forces $\mathbf{f}$ are zero, and the deformation is driven by a Dirichlet boundary condition imposed on the moving boundary.

After discretization, Equation 1.20 must hold for any test function $\psi$, and can therefore be rewritten as a set of equations,

$$\begin{aligned}\mathbf{R}_\mathrm{x} = \sum_\mathrm{e}\int_{\Omega_\mathrm{e}}\left[\frac{E_\mathrm{e}\nu_\mathrm{e}}{2(1+\nu_\mathrm{e})(1-2\nu_\mathrm{e})}\partial_{x_k}N_l\Delta x_{l,k}\delta_{ij} + \frac{E_\mathrm{e}}{2(1+\nu_\mathrm{e})}\left(\partial_{x_j}N_l\Delta x_{l,i}+\partial_{x_i}N_l\Delta x_{l,j}\right)\right]\partial_{x_j}N_l\,dV_\mathrm{e} \\ = 0.\end{aligned} \tag{1.22}$$

The Dirichlet boundary condition on the deforming surface are enforced as,

$$\overline{\Delta x_{i,j}}|_{\Gamma_\mathrm{b}} = \Delta x_{\mathrm{b}_{i,j}}. \tag{1.23}$$

On the wake, the periodic boundary conditions are discretized as follows. The upper wake volume element contributions are added to the lower wake equations, and the upper wake unknowns are prescribed to match the lower wake unknowns,

$$\begin{aligned}
&\sum_{\mathrm{e}} \int_{\Omega_{\mathrm{w,l_e}}} \left[ \frac{E_{\mathrm{e}}\nu_{\mathrm{e}}}{2(1+\nu_{\mathrm{e}})(1-2\nu_{\mathrm{e}})} \partial_{x_k} N_l \Delta x_{l,k} \delta_{ij} + \frac{E_{\mathrm{e}}}{2(1+\nu_{\mathrm{e}})} \left( \partial_{x_j} N_l \Delta x_{l,i} + \partial_{x_i} N_l \Delta x_{l,j} \right) \right] \partial_{x_j} N_l \, dV_{\mathrm{e}} \\
+&\sum_{\mathrm{e}} \int_{\Omega_{\mathrm{w,u_e}}} \left[ \frac{E_{\mathrm{e}}\nu_{\mathrm{e}}}{2(1+\nu_{\mathrm{e}})(1-2\nu_{\mathrm{e}})} \partial_{x_k} N_l \Delta x_{l,k} \delta_{ij} + \frac{E_{\mathrm{e}}}{2(1+\nu_{\mathrm{e}})} \left( \partial_{x_j} N_l \Delta x_{l,i} + \partial_{x_i} N_l \Delta x_{l,j} \right) \right] \partial_{x_j} N_l \, dV_{\mathrm{e}} \\
=&\, 0, \\
&\Delta x_{i,j}|_{\Gamma_{\mathrm{w,u}}} - \Delta x_{i,j}|_{\Gamma_{\mathrm{w,l}}} = 0.
\end{aligned} \tag{1.24}$$

# 2 Partial gradients

This section presents the formulation of the discretized gradients of the full potential and mesh morphing equations. Note that the summation symbol has been dropped for conciseness.

## 2.1 Full potential

This section details the formulation of the partial gradients of full potential equation, and of the aerodynamic loads.

### 2.1.1 Residuals

The partial gradient of the potential residuals with respect to the potential variables, also known as the flow Jacobian, is given by,

$$\begin{aligned}\frac{\partial R_{\phi,i}}{\partial \phi_j} &= J_{\phi,ij} \\ &= \int_{\Omega_\mathrm{e}} (1-\mu)\left[-M_\infty^2 \rho_\mathrm{e}^{2-\gamma} \partial_{x_k}\phi \partial_{x_k} N_j \partial_{x_k}\phi \partial_{x_k} N_i + \rho_\mathrm{e} \partial_{x_k} N_j \partial_{x_k} N_i\right]\, dV_\mathrm{e} \\ &+ \int_{\Omega_\mathrm{e}} \mu \left[-M_\infty^2 \rho_\mathrm{U}^{2-\gamma} \partial_{x_k}\phi_\mathrm{U} \partial_{x_k} N_{\mathrm{U},j} \partial_{x_k}\phi \partial_{x_k} N_i + \rho_\mathrm{U} \partial_{x_k} N_j \partial_{x_k} N_i\right]\, dV_\mathrm{e} \\ &- \int_{\Omega_\mathrm{e}} (\rho_\mathrm{e} - \rho_\mathrm{U}) \left[\frac{2\mu_\mathrm{C} M_\mathrm{C}^2}{M_\mathrm{e}^3}\left(\frac{1}{\sqrt{\partial_{x_k}\phi^2 a_\mathrm{e}^2}} + \frac{\gamma-1}{2}\frac{\sqrt{\partial_{x_k}\phi^2}}{\sqrt[3]{a_\mathrm{e}^2}}\right) \partial_{x_k}\phi \partial_{x_k} N_j \partial_{x_k}\phi \partial_{x_k} N_i\right]\, dV_\mathrm{e},\end{aligned} \tag{2.1}$$

where $a_\mathrm{e}$ is the speed of sound on an element computed as

$$a_\mathrm{e} = \sqrt{\frac{1}{M_\infty^2} + \frac{\gamma-1}{2}(1-|\nabla\phi|^2)}. \tag{2.2}$$

Note that, similar to the residuals $\mathbf{R}_\phi$, the Kutta condition is enforced by adding the contributions of the upper wake nodes to the lower wake rows, instead of the upper wake rows, in the Jacobian matrix,

$$J_{\phi,ij}|_\mathrm{w,l} = J_{\phi,ij}|_\mathrm{w,l} + J_{\phi,ij}|_\mathrm{w,u}. \tag{2.3}$$

The following terms are then assembled on the upper wake rows,

$$J_{\phi,ij}|_\mathrm{w,u} = 2\int_{\Gamma_\mathrm{we}} \left(N_i + \frac{h}{2}\tilde{U}_{\infty,k}\partial_{x_k} N_i\right)_\mathrm{w,u} \left(\left[\partial_{x_k}\phi\partial_{x_k} N_j\right]_\mathrm{w,u} - \left[\partial_{x_k}\phi\partial_{x_k} N_j\right]_\mathrm{w,l}\right)\, dS_\mathrm{e}. \tag{2.4}$$

The partial gradient of the potential residuals with respect to the mesh coordinates is given by,

$$
\begin{aligned}
\frac{\partial R_{\phi,i}}{\partial x_j} = &\int_{\Omega_\mathrm{e}} (1-\mu)\left(-M_\infty^2 \rho_\mathrm{e}^{2-\gamma} \partial_{x_l}\phi \left(-J^{-1}_{\mathrm{e},lk}\partial_{x_j} J_{\mathrm{e},kl}\right)\partial_{x_l}\phi\right)\partial_{x_k}\phi\partial_{x_k}N_i \, dV_\mathrm{e} \\
&+ \int_{\Omega_\mathrm{e}} \mu\left(-M_\infty^2 \rho_\mathrm{U}^{2-\gamma} \partial_{x_l}\phi_\mathrm{U} \left(-J^{-1}_{\mathrm{U},lk}\partial_{x_j} J_{\mathrm{U},kl}\right)\partial_{x_l}\phi_\mathrm{U}\right)\partial_{x_k}\phi\partial_{x_k}N_i \, dV_\mathrm{e} \\
&+ \int_{\Omega_\mathrm{e}} \left[(1-\mu)\rho_\mathrm{e} + \mu\rho_\mathrm{U}\right]\left[\partial_{x_l}\phi\left(-J^{-1}_{\mathrm{e},lk}\partial_{x_j} J_{\mathrm{e},kl}\right)\partial_{x_l}N_i + \partial_{x_l}N_i\left(-J^{-1}_{\mathrm{e},lk}\partial_{x_j} J_{\mathrm{e},kl}\right)\partial_{x_l}\phi\right] dV_\mathrm{e} \\
&- \int_{\Omega_\mathrm{e}} (\rho_\mathrm{e} - \rho_\mathrm{U})\left[\frac{2\mu_\mathrm{C} M_\mathrm{C}^2}{M_\mathrm{e}^3}\left(\frac{1}{\sqrt{\partial_{x_k}\phi^2 a_\mathrm{e}^2}} + \frac{\gamma-1}{2}\frac{\sqrt{\partial_{x_k}\phi^2}}{\sqrt[3]{a_\mathrm{e}^2}}\right)\partial_{x_l}\phi\left(-J^{-1}_{\mathrm{e},lk}\partial_{x_j} J_{\mathrm{e},kl}\right)\partial_{x_l}\phi\partial_{x_k}\phi\partial_{x_k}N_i\right] dV_\mathrm{e} \\
&+ \int_{\Omega_\mathrm{e}} \left[(1-\mu)\rho_\mathrm{e} + \mu\rho_\mathrm{U}\right]\partial_{x_k}\phi\partial_{x_k}N_i \, \partial_{x_j} dV_\mathrm{e}.
\end{aligned}
\tag{2.5}
$$

The partial gradient of the Jacobian matrix of an element with respect to the mesh coordinates is computed as,

$$
\partial_{x_k} J_{\cdot,ij} = \frac{\partial}{\partial_{x_k}}\partial_{\xi_j} N_l x_{l,i}, \tag{2.6}
$$

where $\cdot$ refers to a variable evaluated on the current element $\mathrm{e}$ or on the upstream element $\mathrm{U}$. Since Gauss quadrature is used to compute the integrals in the finite elements method, computing the partial gradient of an elementary volume with respect to the mesh coordinates amounts to computing the partial gradient of the Jacobian matrix determinant of an element as,

$$
\partial_{x_k} dV_\mathrm{e} = \partial_{x_k}\det(J_{\mathrm{e},ij}) = \det(J_{\mathrm{e},ij})\mathrm{tr}(J^{-1}_{\mathrm{e},ij}\partial_{x_k} J_{\mathrm{e},ij}). \tag{2.7}
$$

The contributions of the farfield boundary condition are not taken into account since the outer boundary is fixed. The partial gradient of the wake boundary conditions with respect to the mesh coordinates are assembled in a similar way as the flow residuals: the contributions of the upper wake rows are first added to the lower wake rows, and the upper wake rows are then computed as,

$$
\begin{aligned}
\frac{\partial R_{\phi,i}}{\partial x_j}|_{\mathrm{w,u}} = &\int_{\Gamma_{\mathrm{we}}} \left(\partial_{x_j}\left(\frac{h}{2}\tilde{U}_{\infty,k}\partial_{x_k}N_i\right)\right)_{\mathrm{w,u}} \left(\left[\partial_{x_k}\phi\partial_{x_k}\phi\right]_{\mathrm{w,u}} - \left[\partial_{x_k}\phi\partial_{x_k}\phi\right]_{\mathrm{w,l}}\right) dS_\mathrm{e} \\
&+ 2\int_{\Gamma_{\mathrm{we}}} \left(N_i + \frac{h}{2}\tilde{U}_{\infty,k}\partial_{x_k}N_i\right)_{\mathrm{w,u}} \left[\partial_{x_l}\phi\left(-J^{-1}_{\mathrm{e},lk}\partial_{x_j} J_{\mathrm{e},kl}\right)\partial_{x_l}\phi\right]_{\mathrm{w,u}} dS_\mathrm{e} \\
&- 2\int_{\Gamma_{\mathrm{we}}} \left(N_i + \frac{h}{2}\tilde{U}_{\infty,k}\partial_{x_k}N_i\right)_{\mathrm{w,u}} \left[\partial_{x_l}\phi\left(-J^{-1}_{\mathrm{e},lk}\partial_{x_j} J_{\mathrm{e},kl}\right)\partial_{x_l}\phi\right]_{\mathrm{w,l}} dS_\mathrm{e} \\
&+ \int_{\Gamma_{\mathrm{we}}} \left(N_i + \frac{h}{2}\tilde{U}_{\infty,k}\partial_{x_k}N_i\right)_{\mathrm{w,u}} \left(\left[\partial_{x_k}\phi\partial_{x_k}\phi\right]_{\mathrm{w,u}} - \left[\partial_{x_k}\phi\partial_{x_k}\phi\right]_{\mathrm{w,l}}\right)\partial_{x_j} dS_\mathrm{e},
\end{aligned}
\tag{2.8}
$$

where the first partial gradient can further be developed as,

$$
\partial_{x_j}\left(\frac{h}{2}\tilde{U}_{\infty,k}\partial_{x_k}N_i\right) = \partial_{x_j}\frac{h}{2}\tilde{U}_{\infty,k}\partial_{x_k}N_i + \frac{h}{2}\tilde{U}_{\infty,l}\phi J^{-1}_{\mathrm{e},lk}\partial_{x_j} J_{\mathrm{e},kl}\partial_{x_l}N_i. \tag{2.9}
$$

Computing the partial gradient of an elementary surface with respect to the mesh coordinates amounts to computing the partial gradient of the surface Jacobian matrix determinant of an element. For a two-dimensional surface in a three-dimensional space, this gradient is expressed as,

$$\partial_{x_j} dS_\mathrm{e} = \partial_{x_j} \det(J_{\mathrm{S,e},i}) = \frac{J_{\mathrm{S,e},i}}{|J_{\mathrm{S,e},i}|} \left(\partial_{x_j}\partial_\xi N_k x_k \times \partial_\eta N_k x_k + \partial_\xi N_k x_k \times \partial_{x_j}\partial_\eta N_k x_k\right). \tag{2.10}$$

The angle of attack affects the potential residuals only through the farfield boundary condition. The partial gradient of the potential residuals with respect to the angle of attack is thus given by,

$$\frac{\partial R_{\phi,i}}{\partial \alpha} = \sum_\mathrm{e} \int_{\Gamma_\mathrm{fe}} \rho_\infty \frac{\partial \mathbf{U}_\infty}{\partial \alpha} \cdot \hat{\mathbf{n}}_\mathrm{e} N_i \, dS_\mathrm{e} \tag{2.11}$$

where the gradient of the freestream velocity with respect to the angle of attack is

$$\frac{\partial \mathbf{U}_\infty}{\partial \alpha} = \begin{bmatrix} -\sin\alpha\cos\beta \\ 0 \\ \cos\alpha\cos\beta \end{bmatrix}. \tag{2.12}$$

### 2.1.2 Functional

The partial gradient of the aerodynamic loads with respect to the potential variables is given by,

$$\begin{aligned} \frac{\partial F_i}{\partial \phi_j} &= \frac{1}{2}\rho_\infty u_\infty^2 \int_{\Gamma_\mathrm{b,e}} \partial_{\phi_j} C_{p_\mathrm{e}} \hat{n}_{\mathrm{e},i} \, dS_\mathrm{e} \\ &= -\rho_\infty u_\infty^2 \int_{\Gamma_\mathrm{b,e}} \rho_\mathrm{e}^\gamma \partial_{x_k}\phi \partial_{x_k} N_j \hat{n}_{\mathrm{e},i} \, dS_\mathrm{e}. \end{aligned} \tag{2.13}$$

The partial gradient of the aerodynamic loads with respect to the mesh coordinates is given by,

$$\begin{aligned} \frac{\partial F_i}{\partial x_j} &= \frac{1}{2}\rho_\infty u_\infty^2 \partial_{x_j} \int_{\Gamma_\mathrm{b,e}} C_{p_\mathrm{e}} \hat{n}_{\mathrm{e},i} \, dS_\mathrm{e} \\ &= \frac{1}{2}\rho_\infty u_\infty^2 \left[ \int_{\Gamma_\mathrm{b,e}} -2\rho_\mathrm{e}^\gamma \partial_{x_l}\phi \left(-J^{-1}_{\mathrm{e},lk} \partial_{x_j} J_{\mathrm{e},kl}\right) \partial_{x_l}\phi \hat{n}_{\mathrm{e},i} \, dS_\mathrm{e} \right. \\ &\qquad + \int_{\Gamma_\mathrm{b,e}} C_{p_\mathrm{e}} \partial_{x_j} \hat{n}_{\mathrm{e},i} \, dS_\mathrm{e} \\ &\qquad \left. + \int_{\Gamma_\mathrm{b,e}} C_{p_\mathrm{e}} \hat{n}_{\mathrm{e},i} \, \partial_{x_j} dS_\mathrm{e} \right]. \end{aligned} \tag{2.14}$$

where the partial gradient of an elementary surface is computed as in Eq 2.10, and the partial gradient of the unit normal vector is given by

$$\frac{\partial \hat{n}_i}{\partial x_j} = (I_{ik} - \hat{n}_i \hat{n}_k) \frac{1}{|n_k|} \partial_{x_j} n_k \tag{2.15}$$

where the partial gradient of the normal vector to a two-dimensional triangular area in a three-dimensional space is given by,

$$\frac{\partial \mathbf{n}}{\partial x_j} = \partial_{x_j} \left( \mathbf{x}_1 - \mathbf{x}_0 \right) \times \left( \mathbf{x}_2 - \mathbf{x}_0 \right) + \left( \mathbf{x}_1 - \mathbf{x}_0 \right) \times \partial_{x_j} \left( \mathbf{x}_2 - \mathbf{x}_0 \right). \tag{2.16}$$

The partial gradients of the aerodynamic load coefficients can be readily obtained from Equations 2.13 and 2.14. Additionally, the partial gradients of the aerodynamic coefficients with respect to the angle of attack is given by,

$$\frac{C_L}{\partial \alpha} = \mathbf{C_F} \cdot \frac{\partial \mathbf{e_L}}{\partial \alpha}, \qquad \frac{C_D}{\partial \alpha} = \mathbf{C_F} \cdot \frac{\partial \mathbf{e_D}}{\partial \alpha}, \tag{2.17}$$

where the gradients of the directions are defined as,

$$\frac{\partial \mathbf{e_L}}{\partial \alpha} = \begin{bmatrix} -\cos\alpha \\ 0 \\ -\sin\alpha \end{bmatrix}, \qquad \frac{\partial \mathbf{e_D}}{\partial \alpha} = \begin{bmatrix} -\sin\alpha\cos\beta \\ 0 \\ \cos\alpha\cos\beta \end{bmatrix}. \tag{2.18}$$

## 2.2 Mesh deformation

This section details the formulation of the partial gradients of mesh morphing equations.

### 2.2.1 Residuals

The mesh deformation residuals only depend linearly on the mesh coordinates. The partial gradients of the mesh deformation residuals with respect to the mesh coordinates, also known as the mesh Jacobian, is therefore given by,

$$\begin{aligned} \frac{\partial R_{\mathrm{x},i}}{\partial x_j} &= J_{\mathrm{x},ij} \\ &= \sum_{\mathrm{e}} \int_{\Omega_\mathrm{e}} \left[ \frac{E_\mathrm{e}\nu_\mathrm{e}}{2(1+\nu_\mathrm{e})(1-2\nu_\mathrm{e})} \partial_{x_k} N_l \delta_{ij} + \frac{E_\mathrm{e}}{2(1+\nu_\mathrm{e})} \left( \partial_{x_j} N_l + \partial_{x_i} N_l \right) \right] \partial_{x_j} N_l \, dV_\mathrm{e}. \end{aligned} \tag{2.19}$$

Note that, similar to the residuals $\mathbf{R}_\mathrm{x}$, periodic boundary conditions are prescribed on the wake by adding the upper wake volume element contributions to the lower wake equations, and by prescribing the upper wake unknowns to match the lower wake unknowns.

# 3 Solution procedures

This section presents the direct and adjoint solution procedures that are readily available in `DART`. If multiphysics computations are to be performed, the interfaces for `CUPyDO` [5, 6, 7] and `openMDAO` [8, 9] can be used.

## 3.1 Direct solution

The full potential equation being nonlinear, it needs to be solved in an iterative fashion. A Taylor expansion around a solution vector $\boldsymbol{\phi}_\mathrm{s}$ allows to write

$$0 = \mathbf{R}_\phi + \frac{\partial \mathbf{R}_\phi}{\partial \boldsymbol{\phi}} \boldsymbol{\Delta\phi} + \mathcal{O}(\boldsymbol{\Delta\phi}^2), \tag{3.1}$$

where $\boldsymbol{\Delta\phi} = \boldsymbol{\phi} - \boldsymbol{\phi}_\mathrm{s}$. Neglecting second order terms, and given a known solution estimate $\boldsymbol{\phi}_n$ at iteration $n$, a better estimate of the solution, $\boldsymbol{\phi}_{n+1}$, can be found by solving

$$\frac{\partial \mathbf{R}_\phi}{\partial \boldsymbol{\phi}}|_{\boldsymbol{\phi}_n} (\boldsymbol{\phi}_{n+1} - \boldsymbol{\phi}_n) = -\mathbf{R}_\phi|_{\boldsymbol{\phi}_n}. \tag{3.2}$$

The Newton-Raphson method exhibits a second-order convergence rate as it gets closer to the solution. However, it might be unstable for transonic flow computations where the local Mach numbers are high. An effective way to stabilize the Newton method is to restrict the change in the solution using a line search procedure. In such a technique, the new solution vector is computed as

$$\boldsymbol{\phi}_{n+1} = \boldsymbol{\phi}_n + s_n(\boldsymbol{\phi}_{n+1} - \boldsymbol{\phi}_n), \tag{3.3}$$

where $s_n$ is the step length of the line search. The Bank and Rose [10] algorithm has been implemented to find the optimal step length for a given iteration.

## 3.2 Adjoint solution

An adjoint method has also been implemented to compute the total gradients of the lift and the drag with respect to the angle of attack and the surface grid coordinates. These gradients can then be used in an optimization process. For pure aerodynamic optimization, the problem can be formulated as follows,

$$\begin{aligned} &\min_{\mathbf{x},\alpha} F_\mathrm{obj}(\boldsymbol{\phi}, \mathbf{x}, \alpha) \\ &\text{s.t. } \mathbf{R}_\phi = 0 \\ &\qquad \mathbf{R}_\mathrm{x} = 0 \end{aligned} \tag{3.4}$$

where $\boldsymbol{\phi}$ denote the vector of aerodynamic potential variables, $\alpha$ is the angle of attack, $\mathbf{R}_\phi$ represents the full potential equation noted in residual form, and $F_\mathrm{obj}$ is the functional (lift or drag) to be minimized. Since a nonlinear aerodynamic model is used, the full potential equations must be solved in the volume surrounding the geometry, which will deform according to follow the movement of the surface grid. In such a case, it is also convenient to explicitly introduce the vector of volume mesh coordinates, $\mathbf{x}$, and the mesh morphing laws residuals, $\mathbf{R}_{\mathrm{x}}$, into the optimization formulation.

In order to minimize $F_{\mathrm{obj}}$, the augmented Lagrangian $\mathcal{L}$ is first constructed as,

$$\mathcal{L} = F_{\mathrm{obj}} + \boldsymbol{\lambda}_{\phi}\mathbf{R}_{\phi} + \boldsymbol{\lambda}_{\mathrm{x}}\mathbf{R}_{\mathrm{x}} \tag{3.5}$$

and then differentiated such that,

$$\delta\mathcal{L} = 0 \Rightarrow \begin{cases} \frac{\partial F_{\mathrm{obj}}}{\partial \boldsymbol{\phi}} + \boldsymbol{\lambda}_{\phi}\frac{\partial \mathbf{R}_{\phi}}{\partial \boldsymbol{\phi}} + \boldsymbol{\lambda}_{\mathrm{x}}\frac{\partial \mathbf{R}_{\mathrm{x}}}{\partial \boldsymbol{\phi}} = 0 \\ \frac{\partial F_{\mathrm{obj}}}{\partial \mathbf{x}} + \boldsymbol{\lambda}_{\phi}\frac{\partial \mathbf{R}_{\phi}}{\partial \mathbf{x}} + \boldsymbol{\lambda}_{\mathrm{x}}\frac{\partial \mathbf{R}_{\mathrm{x}}}{\partial \mathbf{x}} = 0 \\ \frac{\partial F_{\mathrm{obj}}}{\partial \alpha} + \boldsymbol{\lambda}_{\phi}\frac{\partial \mathbf{R}_{\phi}}{\partial \alpha} + \boldsymbol{\lambda}_{\mathrm{x}}\frac{\partial \mathbf{R}_{\mathrm{x}}}{\partial \alpha} = 0 \\ \mathbf{R}_{\phi} = 0 \\ \mathbf{R}_{\mathrm{x}} = 0 \end{cases} . \tag{3.6}$$

In order to obtain the total gradients of $F_{\mathrm{obj}}$, the nonlinear potential and linear mesh equations, $\mathbf{R}_{\phi} = 0$ and $\mathbf{R}_{\mathrm{x}} = 0$ must first be solved. The coupled set of linear adjoint equations,

$$\begin{bmatrix} \partial_{\boldsymbol{\phi}}\mathbf{R}_{\phi}{}^{\mathrm{T}} & \partial_{\mathbf{x}}\mathbf{R}_{\mathrm{x}}{}^{\mathrm{T}} \\ \partial_{\boldsymbol{\phi}}\mathbf{R}_{\phi}{}^{\mathrm{T}} & \partial_{\mathbf{x}}\mathbf{R}_{\mathrm{x}}{}^{\mathrm{T}} \end{bmatrix} \begin{bmatrix} \boldsymbol{\lambda}_{\phi} \\ \boldsymbol{\lambda}_{\mathrm{x}} \end{bmatrix} = - \begin{bmatrix} \partial_{\boldsymbol{\phi}}F_{\mathrm{obj}}^{\mathrm{T}} \\ \partial_{\mathbf{x}}F_{\mathrm{obj}}^{\mathrm{T}} \end{bmatrix} \tag{3.7}$$

must then be solved for the Lagrange multipliers $\boldsymbol{\lambda}_{\phi}$ and $\boldsymbol{\lambda}_{\mathrm{x}}$. The total gradient with respect to the surface mesh coordinates can readily be recovered from $\lambda_{\mathrm{x}}$, as they are a subset of this vector [11]. The total gradient with respect to the angle of attack can finally be obtained by injecting the solution into

$$\frac{dF_{\mathrm{obj}}}{d\alpha} = \frac{\partial F_{\mathrm{obj}}}{\partial \alpha}^{\mathrm{T}} - \frac{\partial \mathbf{R}_{\phi}}{\partial \alpha}^{\mathrm{T}} \boldsymbol{\lambda}_{\phi}. \tag{3.8}$$

# References

[1] DARTFlo - Discrete Adjoint for Rapid Transonic Flows. https://gitlab.uliege.be/am-dept/dartflo, Accessed October 2021.

[2] Adrien Crovato. *Steady Transonic Aerodynamic and Aeroelastic Modeling for Preliminary Aircraft Design*. PhD thesis, University of Liège, October 2020.

[3] Joseph L. Steger and Barrett S. Baldwin. Shock waves and drag in the numerical calculation of isentropic transonic flows. Technical report, NASA, 1972.

[4] Richard P. Dwight. Robust Mesh Deformation using the Linear Elasticity Equations. *Journal of Computational Fluid Dynamics*, 12:401–406, 2009.

[5] David Thomas, Marco-Lucio Cerquaglia, Romain Boman, Thomas Economon, Juan Alonso, Grigorios Dimitriadis, and Vincent E. Terrapon. CUPyDO: An integrated Python environment for coupled fluid-structure problems. *Advances in Engineering Software*, 2019.

[6] Maerco-Lucio Cerquaglia, David Thomas, Romain Boman, Vincent E. Terrapon, and Jean-Phillipe Ponthot. A fully partitioned Lagrangian framework for FSI problems characterized by free surfaces, large solid deformations and displacements, and strong added-mass effects. *Computer Methods in Applied Mechanics and Engineering*, 2019.

[7] CUPyDO - Python tools for partitioned fluid-structure coupling. http://github.com/ulgltas/cupydo, Accessed October 2021.

[8] Justin S. Gray, John T. Hwang, Joaquim R. R. A. Martins, Kenneth T. Moore, and Bret A. Naylor. OpenMDAO: An open-source framework for multidisciplinary design, analysis, and optimization. *Structural and Multidisciplinary Optimization*, 59(4):1075–1104, April 2019.

[9] openMDAO - An open-source framework for efficient multidisciplinary optimization. https://openmdao.org/, Accessed October 2021.

[10] Randolph E. Bank and Donald J. Rose. Global Approximate Newton Method. *Numerische Mathematik*, 27:179–295, 1981.

[11] Markus Widhalm, Joël Brezillon, Caslav Ilic, and Tobias Leicht. Investigation on Adjoint Based Gradient Computations for Realistic 3d Aero-Optimization. In *13th AIAA/ISSMO Multidisciplinary Analysis Optimization Conference*. AIAA, September 2010.